WATER-VAPOR ESTIMATION FOR OCEAN SCENES USING MODULATED SURFACE REFLECTANCE

Craig Gelpi and Bao Nguyen[1]

1. Introduction

Imaging spectrometers such as AVIRIS gather data in 3 dimensions: an electromagnetic wavelength dimension and 2 spatial dimensions. These latter are usually used to make images depicting the spatial relationship among features found in the electromagnetic spectra. However, the spatial dimensions can be used to organize the spectra according to spatial scale. This can be a powerful tool in the analysis and interpretation of hyperspectral data as different spectra may be realized at different scale lengths. We illustrate this phenomenon with a study of water-vapor estimation using high-altitude hyperspectral data of ocean scenes.

Atmospheric compensation of at-sensor radiance for scattering and absorption to derive intrinsic surface reflectance is a basic task in the analysis of hyperspectral data (Green, 1990; Gao et al., 1993). Compensation for atmospheric water-vapor absorption is particularly important due to the large portion of the reflectance spectrum affected by it. However, conventional hyperspectral techniques (e.g., those employing the continuum interpolated band ratio, CIBR) which accurately estimate the amount of atmospheric water over land scenes (Gao and Goetz, 1990; Carrère and Conel, 1993) grossly underestimate the water content over dark scenes such as the ocean. This is due to atmospheric path scattering distorting the absorption features, making them less distinct by supplying photons that have not propagated through the water-laden lower atmosphere. Hence, when the atmospheric path scattering is a significant component of the total radiance, as when viewing dark surfaces such as the ocean from high-altitude platforms, conventional water-vapor estimation techniques are less effective.

However, photons which have traversed the entire distance from the sun to the sensor via the ocean surface have imprinted on them the surface modulations produced by ocean waves. These waves exhibit strong energy at scale lengths smaller than 500 m, a regime where we expect little atmospheric contribution but that is easily resolved with the sampling capability of many imaging spectrometers. Through a decomposition of the hyperspectral cube into spatial spectra, we can separate some of those photons which have interacted with the surface from those that haven't, and construct a spectrum which has no atmospheric path-scattered radiance contributions. Conventional techniques to estimate water-vapor operating on this new spectrum should work well.

In the following section we describe the Modulated Surface Reflectance (MSR) algorithm which is designed to take advantage of the short scales of ocean waves in the computation of water vapor. Using AVIRIS data for the Santa Barbara Channel we present water-vapor column density obtained from the algorithm for over-ocean scenes. Although we do not have an independent measure of atmospheric water vapor we assume that conventional techniques as incorporated into computer software such as ATREM (ATmospheric REMoval, Gao et al., 1997) provide truth when used for bright targets such as land. ATREM values obtained over the coastline and islands are used to infer oceanic values via interpolation and extrapolation and these values are compared to those retrieved from the MSR algorithm.

2. Algorithm Implementation and Verification

As an illustration of the MSR technique we compute the MSR electromagnetic spectrum and derive water-vapor column density from it. We use AVIRIS data from flight line f970414t01p02_r02 (33'52''N, -120'08''E, site name CALCOFI) which made measurements from the Santa Barbara Channel off the coast of California, south across Santa Rosa Island and out into the Pacific Ocean. As a demonstration below we compute the horizontal profile of the column density across adjacent land and sea areas, noting the effect of path scattering relative to the background brightness. Typical radiance spectra for

[1] XonTech, Inc., 6862 Hayvenhurst Ave. Van Nuys, California 91406, USA
craig_gelpi@xontech.com

ocean and land areas are shown in Figure 1. The land spectrum is for Santa Rosa Island and the ocean spectrum is for adjacent Santa Barbara Channel using the same solar and view geometry. Over this near-infrared region, the ocean radiance is approximately 10% that of the land value and the atmospheric path scattering is expected to a significant component of the at-sensor radiance.

Data for the 1.14 μm wavelength channel for a 2300 m/side square are shown in the top panel in Figure 2. Although these data have been corrected for the sensor geometry and mapped to a uniform cell size of 18 m/side, this preparation usually is not required. However, standard data pre-processing in preparation for Fourier transformation is necessary, including detrending, tapering and perhaps the editing of outliers produced by breaking waves, all with the intent of minimizing processing sidelobes of long wavelength components which contain the path radiance. For our example, we performed a high-pass filter which passed all wavelengths shorter than 275 m. The size of the area used in the Fourier transform is chosen for the granularity of the desired water-vapor estimates as well as for the spectral resolution required to separate path-scattering and ocean wave modulations. The resulting power spectral density is shown in the bottom panel of Figure 2. It exhibits 2 strong peaks, one corresponding to a wavelength of 100 m and the other to a wavelength of 250 m. These peaks correlate with peaks in the waveheight spectra as reported by a nearby NOAA buoy.

Power spectra are computed for every electromagnetic wavelength. The wavenumber of the peak in power outside a low-wavenumber exclusion region is found for a particular band (for our case a water-vapor absorption band) and a spectrum is formed using the power at this wavenumber for every band as illustrated in Figure 3. We call the resulting spectrum the MSR spectrum. The MSR spectrum has different characteristics than the individual spectra from which it is derived. It does not include significant contributions from atmospheric path scattering or upwelling, water-column radiance. As a consequence, atmospheric absorption features are more distinct. This is illustrated in Figure 4 where we have averaged spectra over land and water off the coast of California and normalized each by the radiance in the 0.94 μm band. Clearly, the absorption features are more pronounced in the land spectrum. Similarly, we have added the MSR spectrum, derived from the same data as the average ocean spectrum. The MSR values correspond very well to the shape of the land spectrum and accordingly, will produce a similar value for the amount of water vapor.

The water-vapor column density can be computed directly from the MSR spectra, producing one value for the area over which the Fourier transform was taken. We scaled the MSR spectrum to the average spectrum value at the 0.875 μm band. This scaled MSR spectrum is input into ATREM and the water vapor computed. We show in Figure 5 the average water-vapor amounts as deduced from the original spectra and the amount obtained from the MSR spectra for either side of Santa Rosa Island as well as the average for the island. From the original spectra ATREM computes 1.9 gm/cm^2 precipitable water over the island and 1.2 gm/cm^2 over the adjacent waters. This difference between land and ocean values is a result of the dark ocean reflectivity. Results obtained over the ocean from the MSR spectrum, 1.9 gm/cm^2, are similar to those obtained over the island from the average spectra. This similarity of these results verify the usefulness of over-ocean, water-vapor retrieval with the MSR technique.

3. Summary and Discussion

We computed the true absorption depth of the water-vapor absorption features using the MSR spectrum. Knowing the true depth of these features permits calculation of an effective atmospheric reflectivity or path radiance, i.e., the additive radiance needed to transform the true absorption depth into the observed one. This quantity contains important information on the atmosphere. It is related to the aerosol loading; and, when computed for several absorption bands, provides information on the wavelength dependence of the aerosol scattering. Using the assumption that the water vapor is confined to a thin layer along the surface we find for these data that the atmospheric reflectivity at 0.94 and 1.14 μm is 0.0035 and 0.0013, respectively. These values are similar to those expected from Rayleigh scattering in a completely dry atmosphere.

Although we have concentrated on the more sensitive water-vapor absorption bands located at wavelengths of 0.94 and 1.14 μm, the effect is also measurable at other bands such as the O_2 absorption

band at 0.76 μm. Although the smaller width and depth of these other absorption features require more signal-processing prowess, applying the MSR technique to these bands may provide a broader characterization of the atmosphere.

Additionally, the effective path radiance can be subtracted from the original radiance to enable calculation of water-vapor values for every pixel. As an example we employ data from a low-altitude hyperspectral experiment (using the Probe-1) and we compute water vapor for every pixel using the original spectrum and display the resulting field in the top panel of Figure 6. The field exhibits structure produced by apparent surfactant streaks as found in the visible bands (not shown). This structure is unlikely to be real as any small-scale structure produced in the real water-vapor profile by the streaks on the surface will quickly be diffused by the wind. When we remove the path-scattered radiance and re-compute the water-vapor field, the structure correlated with the visible surface features disappears as shown in the bottom panel of Figure 6. These data were acquired specifically to analyze surfactant streaks and applying accurate water-vapor compensation which is independent of the surface brightness is crucial.

Finally, if the modulated reflectivity varies with wavelength in a known way, the relative transmittance for the entire measured spectrum can be retrieved. For the AVIRIS example given here the modulated reflectance is determined by glinting waves. The electromagnetic wavelength dependence as given by Fresnel's relation is small; hence the MSR spectrum is essentially a scaling of the solar spectrum attenuated by the atmospheric transmittance. The wavelength dependence of this transmittance may be discerned via the MSR spectrum.

4. References

Carrère, V. and Conel, J. E. (1993), Recovery of Atmospheric Water Vapor Total Column Abundance from Imaging Spectrometer Data Around 940 nm- Sensitivity Analysis and Application to Airborne Visible/Infrared Imaging Spectrometer (AVIRIS) Data. Remote Sens. Environ. 44:179-204.

Gao, B-C. and Goetz, A.F.H. (1990), Column Atmospheric Water Vapor and Vegetation Liquid Water Retrievals from Airborne Imaging Spectrometer Data. J. Geophys. Res., 95:3549-3564.

Gao, B-C., Heidebrecht, K. B. and Goetz, A. F.H. (1993), Derivation of Scaled Surface Reflectances from AVIRIS Data. Remote Sens. Environ., 44:165-178.

Gao, B-C., Heidebrecht, K. B. and Goetz, A. F.H. (1997), Atmospheric Removal Program (ATREM) Version 3.0 User's Guide. Center for the Study of Earth from Space, University of Colorado, Boulder, CO.

Green, R.O. (1990), Radiative Transfer Based Retrieval of Reflectance from Calibrated Radiance Imagery Measured by an Imaging Spectrometer for Lithological Mapping of the Clark Mountains, California. *SPIE* 1298:213-221.

5. Acknowledgments

This work was sponsored by XonTech's Special Studies Division Internal Research and Development Program. The AVIRIS data were obtained from the Jet Propulsion Laboratory (JPL). The Probe-1 data were provided by the Geosat Committee, Inc.

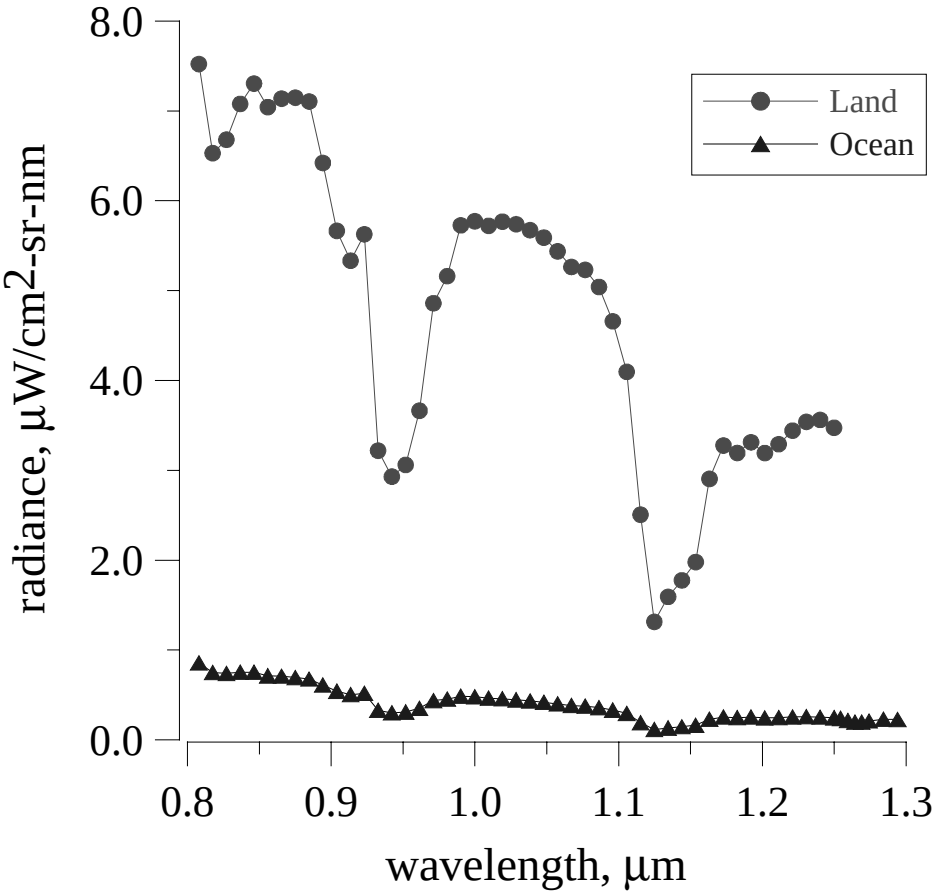

Figure 1. Near-infrared radiance for adjacent land and ocean regions.

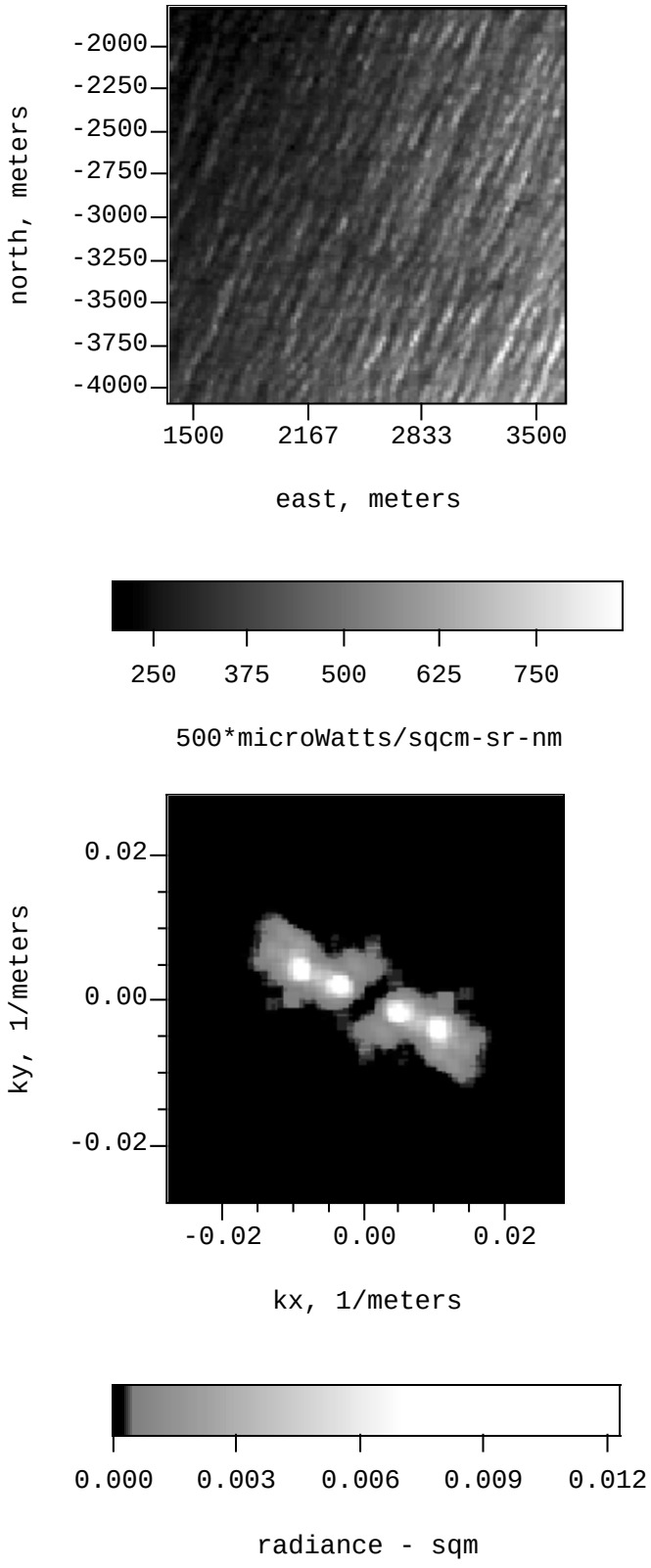

Figure 2. Georectified radiance for subregion of AVIRIS flight f970414t01p02_r02 (top panel). Bottom panel is the corresponding power spectral density.

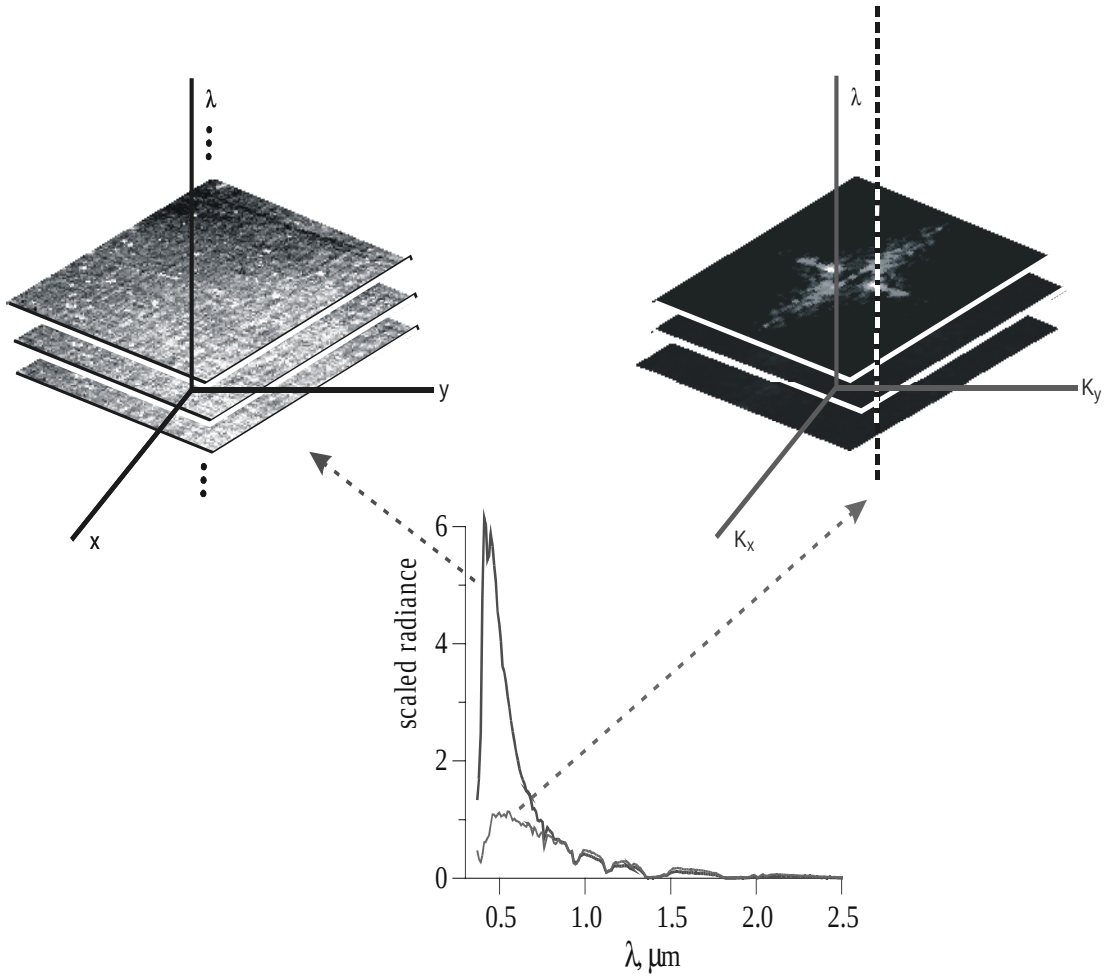

Figure 3. Optical spectra (bottom) scaled to value of band 55 (0.875 μm) obtained from the average of the radiance cube (top left) and the amplitude of the modulated surface reflectance (top right).

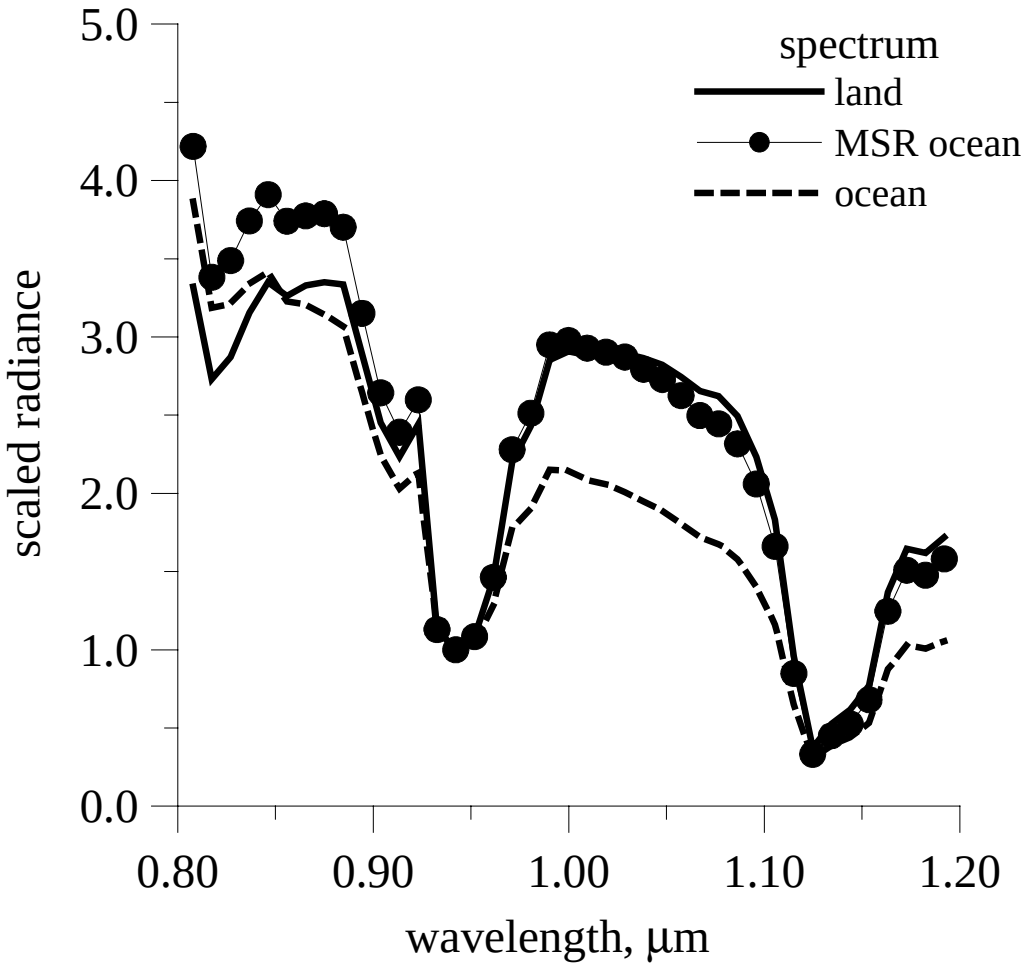

Figure 4. Average NIR land, ocean and MSR-ocean spectra scaled by their respective values at 0.94 μm.

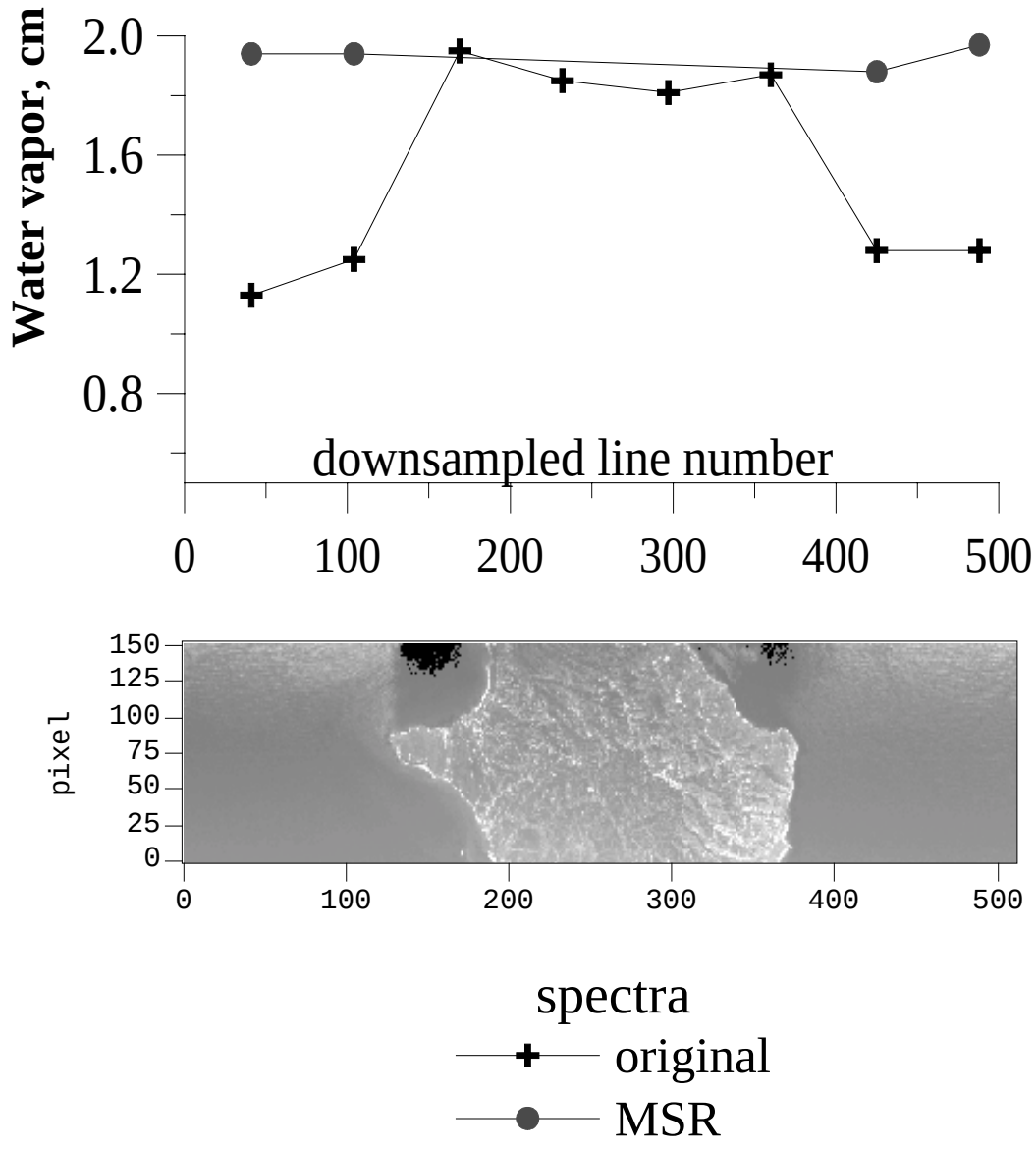

Figure 5. The top panel is the average water vapor amounts (crosses) averaged over 128^2 pixels (not decimated). The closed circles are the water-vapor values obtained from the MSR spectrum computed from the same areas. The bottom panel is an image of Santa Rosa Island with the 0.45 μm band.

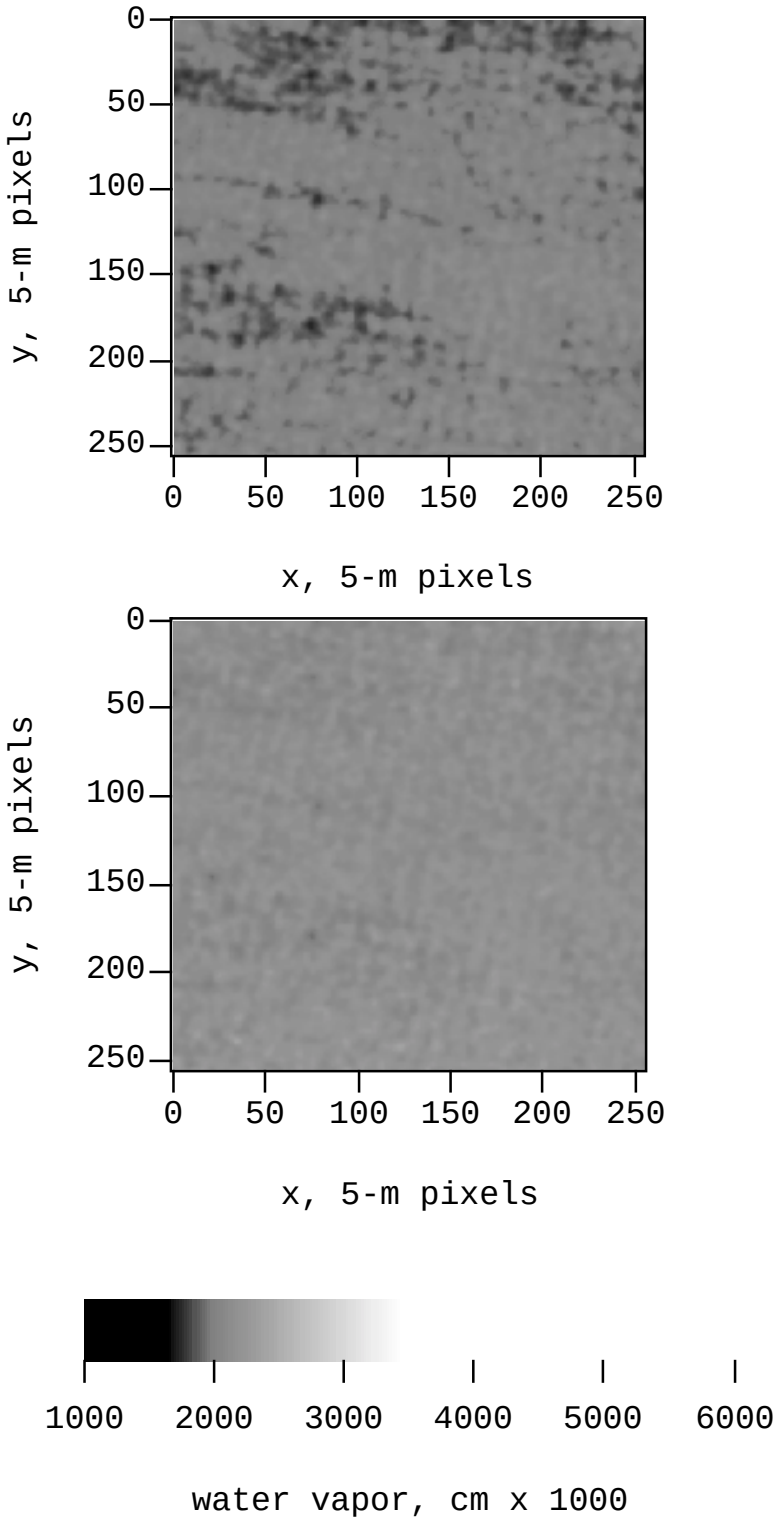

Figure 6. Water-vapor fields computed with original spectra (top) and MSR-derived atmospheric reflectivity (bottom) for ocean region with surfactant streaks. The data used are low-altitude Probe-1 measurements from Hyperspectral Group Shoot 1998.